Nanorobotic Spot Welding: Controlled Metal Deposition with Attogram Precision from Copper-Filled Carbon Nanotubes

Lixin Dong,[†] Xinyong Tao,[‡] Li Zhang,[†] Xiaobin Zhang,[‡] and Bradley J. Nelson*,[†]

Institute of Robotics and Intelligent Systems, ETH Zurich, CH-8092 Zurich, Switzerland, Department of Materials Science and Engineering, Zhejiang University, Hangzhou 310027, China

ABSTRACT

With the continuing development of bottom-up nanotechnology fabrication processes, spot welding can play a role similar to its macro counterpart for the interconnection of nano building blocks for the assembly of nanoelectronics and nanoelectromechanical systems (NEMS). Spot welding using single-crystalline copper-filled carbon nanotubes (CNTs) is investigated experimentally using nanorobotic manipulation inside a transmission electron microscope (TEM). Controlled melting and flowing of copper inside nanotube shells are realized by applying bias voltages between 1.5 and 2.5 V. The average mass flow rate of the copper was found to be 120 ag/s according to TEM video imaging (measured visually at approximately 11.6 nm/s through the CNT). Successful soldering of a copper-filled CNT onto another CNT shows promise for nano spot welding and thermal dip-pen lithography.

With its historic development tracing back to the Bronze Age, welding serves modern industry in broad areas such as construction, manufacturing, and engineering. Spot welding, a widely used resistance welding process, was originally developed by Elihu Thompson in the early 1900s.[1] The most common application of spot welding is in the automobile industry, where it is widely used and most often performed automatically by preprogrammed industrial robots on assembly lines. With the continuing development of bottom-up nanotechnology fabrication processes, spot welding may likewise play an important role in interconnecting carbon nanotubes (CNTs),[2] nanowires,[3] nanobelts,[4] nanohelixes,[5] and other nanomaterials and structures for the assembly of nanoelectronics and nanoelectromechanical systems (NEMS).

Van der Waals forces,[6] electron-beam-induced deposition (EBID),[7] focused-ion-beam chemical vapor deposition (FIB-CVD),[8] high-intensity electron-beam welding,[9] Joule-heating-induced joining,[10] and nanomechanochemical bonding[11] are experimentally demonstrated interconnection strategies, although all have limitations. Van der Waals forces are generally very weak, Joule-heating-induced joining[10] and nanomechanochemical bonding[11] are promising but not yet mature, and the other methods involve high-energy electron or ion beams, which significantly limits their applications. Another interconnection approach is to use CNTs, with their hollow cores and large aspect ratios,[12,13] as possible conduits for nanoscale amounts of various materials that can be used to fuse CNTs together. A variety of materials have been encapsulated by CNTs such as metals and their compounds,[14−16] water,[12] and fullerenes,[17] and applications of devices such as templates,[18] thermometers,[19] and nano test tubes[20] have been presented. The possibility to deliver[21] encapsulated materials from carbon shells is of great interest because of potential applications as sources of small numbers of atoms for nanoprototyping, nanoassembly, and injection. Recently, novel CNTs filled with single-crystalline Cu-nanoneedles have been synthesized by a thermal CVD method using alkali-modified copper catalysts.[22] Because copper is a good conductor of heat and electricity and has a very low binding energy (0.1−0.144 eV/atom) when bound to carbon, encapsulated copper inside nanotubes is ideal for many of these potential applications. Here we present an experimental investigation of controlled melting and flowing of single-crystalline copper from CNTs assisted by nanorobotic manipulation[6] and its application in spot welding of nanotubes using this copper.

The CNT samples were synthesized using an alkali-doped Cu catalyst by a thermal CVD method.[22] Parts a−d of Figure 1 show their structures imaged by field emission scanning

* Corresponding author. E-mail: bnelson@ethz.ch.
† Institute of Robotics and Intelligent Systems, ETH Zurich.
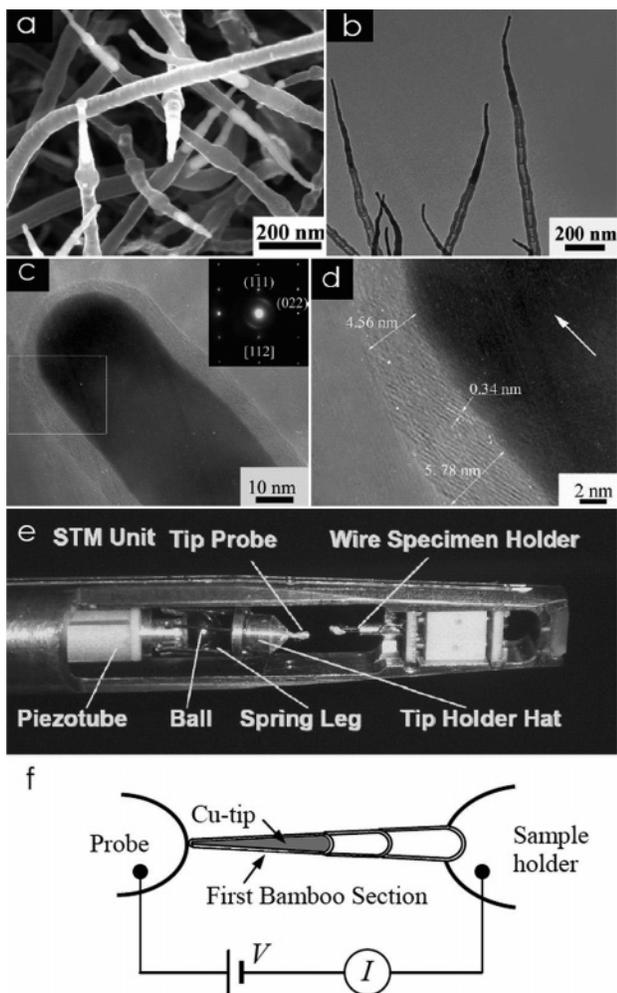‡ Department of Materials Science and Engineering, Zhejiang University.

Figure 1. (a−d) Copper-filled CNTs. (a) FESEM images of Cu-filled CNTs. Observation shows that all the CNTs have sharp tips filled with metal nanoneedles. These CNTs are up to 5 μm long, with outer diameters in a range of 40−80 nm. (b) A typical copper-filled CNT synthesized for 30 min. (c) HRTEM image reveals that the Cu nanoneedles are encapsulated in graphite walls approximately 4−6 nm thick. The inset is the corresponding SAED pattern of the Cu nanoneedle along the [112] zone axis, showing that the Cu nanoneedle is single crystalline. The appearance of a pair of arcs in the SAED pattern indicates some orientation of the (002) planes in the carbon tubes. (d) The magnified image of the rectangular region in (c). The large arrows indicate the growth direction of the CNTs. The interlayer spacing of carbon nanotube is about 0.34 nm, consistent with the (002) plane lattice parameter of graphite. It can also be seen that the graphite layers are not parallel to the tube axis. (e,f) Nanorobotic manipulation system in a TEM. (e) ST1000 STM-TEM holder (Nanofactory Instruments AB). (f) Schematic setup.

electron microscopy (FESEM, Sirion, FEI), TEM (JEM-2010, 200 kV), selected area electron diffraction (SAED), and high-resolution TEM (HRTEM). It can be seen from these observations that the yield of the Cu-filled CNTs was high. The CNTs were up to 5 μm long with outer diameters in a range of 40−80 nm. The single-crystalline Cu nano-needles were encapsulated in graphite walls approximately 4−6 nm thick in the first sections of the bamboo-structured CNTs. The graphite layers were not parallel to the tube axis.

Our experiments were performed in a CM30 TEM equipped with a scanning tunneling microscope (STM)

fabricated in a TEM holder[23] (Nanofactory Instruments AB, ST-1000) serving as a manipulator, as shown in parts e and f of Figure 1. The material consisting of a CNT bundle was attached to a 0.35 mm thick Au wire using silver paint, and the wire was held in the specimen holder. The probe was an etched 10 μm thick tungsten wire with a tip radius of approximately 100 nm (Picoprobe, T-4−10-1 mm). The probe can be positioned in a millimeter-scale workspace with subnanometer resolution with the STM unit actuated by a three-degree-of-freedom piezotube,[23] making it possible to select a specific CNT. Physical contact can be made between the probe and the tip of a nanotube. Applying a voltage between the probe and the sample holder establishes an electrical circuit through a CNT and injects thermal energy into the system via Joule heating. By increasing the applied voltage, the local temperature can be increased past the melting point of the copper encapsulated in a tube. The process was recorded by TEM images and real-time video.

Figure 2 shows transmission electron microscope (TEM) images of melting and flowing copper inside the carbon shells of a Cu-filled CNT. The tip of a Cu-filled CNT was first brought into contact with the tungsten probe (Figure 2a). Then a bias voltage was applied on the two ends of the CNT, with the tungsten probe serving as the anode. The voltage was slowly increased from 0 mV with 100 mV steps. When the voltage reached 1500 mV, a vacant section inside the carbon shells appeared, indicating that the copper has begun melting (Figure 2b). Transportation of the copper to the probe-tip contact moved the vacant section to the root of the first bamboo section of the Cu-filled CNT (Figure 2c). After the vacant section reached the root, the copper core started to flow to the tip of the CNT when bias was increased to 2500 mV. After all the copper flowed out, the probe was moved away from the CNT while keeping the bias on (Figure 2d). A sphere is visible on the tip of the CNT (see inset for a high magnification image), suggesting the formation is related to a melting process. Applying an image processing routine to the data from these experiments, we calculated that the Cu-filled section has an external diameter of approximately 52 nm at the root and 30 nm near the tip, whereas the original Cu core has a diameter of about 39 and 22 nm and a length of 874 nm. The diameter of the copper sphere is 49 nm. Therefore, we determined the mass of the original copper core is approximately 6 fg (femtograms), and the resulting sphere is 0.5 fg according to the density of copper (8.92 g cm^{-3}). We deduce that the missing mass (91%) diffused onto the tungsten probe.

The entire process was recorded with real-time TEM imaging. Figure 2e shows selected video frames of the melting process. The first vacant section (Figure 2b) formed at 48 s, and the second one (Figure 2c) at 86 s. The vacant section then moved to the bottom of the first bamboo section of the CNT. Current vs voltage curves were obtained (Figure 2f) during the process, showing an obvious current drop at 1500 mV as melting began, which we attribute to resistance increases of the tube due to increased temperature. It can also be seen that under −1500 mV the current was larger than that under −1400 mV, which could be a result of the
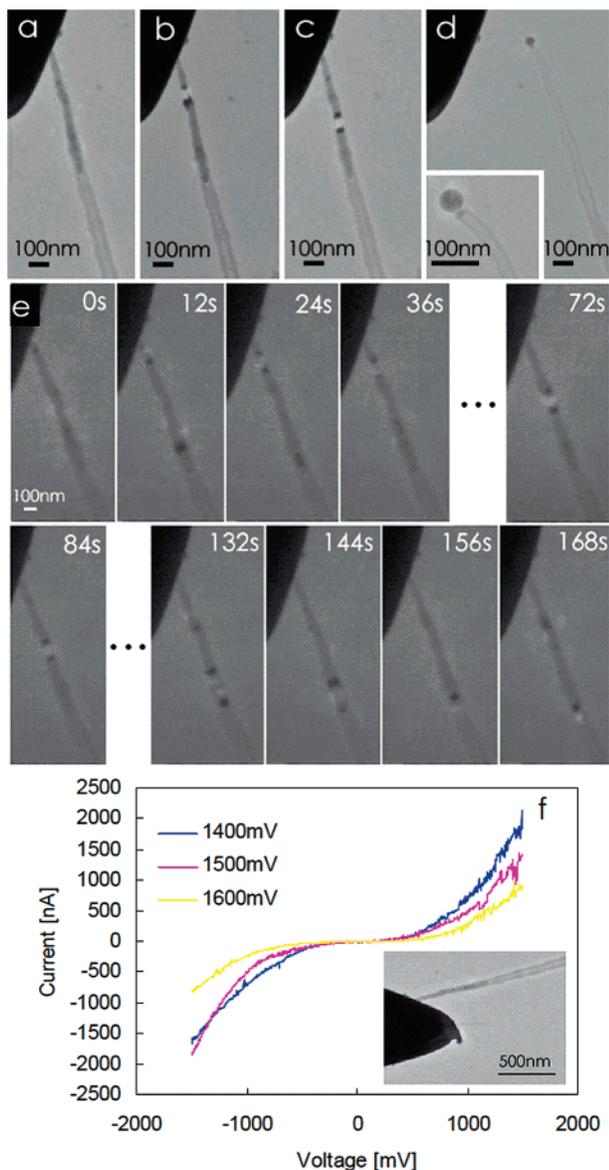
Figure 2. TEM images of melting and flowing of copper inside carbon shells. (a) A Cu-filled CNT was brought into contact with a tungsten probe. (b,c) Under a 1.5 V bias, a vacant section appeared and moved to the root of the first bamboo section of the Cu-filled CNT, showing the melting occurred, after which the copper started to flow to the tip of the CNT under a 2.5 V bias. (d) After all the copper flowed out, the probe was moved away from the CNT. A sphere is visible on the tip of the CNT (see inset for a high magnification image). The Cu-filled section has an external diameter of ca. 52 nm at the root and ca. 30 nm near the tip, whereas the Cu core has a diameter of ca. 39 and 22 nm, respectively. The diameter of the copper sphere is ca. 49 nm. (e) Time-resolved TEM images from video frames showing the melting process. The first vacant section (Figure 2b) formed at 48 s, and the second one (Figure 2c) at 86 s. The vacant section then moved to the bottom of the first bamboo section of the CNT. Obvious melting occurred when the bias voltage reached 1500 mV from 0 mV with 100 mV steps. (e) Current vs voltage curves were obtained during the process, showing an obvious current drop at 1500 mV as melting began, which we attribute to resistance increases of the tube due to the increased temperature. It can also be seen that, under −1500 mV, the current is larger than that under −1400 mV, which could be a result of the decrease of the contact resistance between the nanotubes and the probe due to the flowed out of copper. Inset of (f) shows the configuration of I−V characterization.

decrease of the contact resistance between the nanotube and the probe due to the copper flowing from the tube onto the probe or improved tunneling through a nonideal contact.

The melting was due to Joule heating of the copper by the transport current and electron beam bombardment by the TEM. The irradiation of the electrons can cause the temperature increase of the sample due to inelastic scattering, but because of the low intensity of the beam and the short time, electron beam bombardment is not the main mechanism. Also, no melting or morphology changes of the copper core have been observed before applying the bias voltage, therefore, we attribute transportation current-induced Joule heating to be the main factor. The current can be readily controlled by adjusting the external voltage, which makes this approach easily applied in NEMS, because the process does not require a high energy beam source.

Figure 3a is a series of time-resolved TEM images taken from video frames showing the flowing process. The copper core started to flow inside the carbon shell from the bottom to the tip of the first bamboo section as the bias voltage reached 2.5 V. The entire process continued for about 70 s. The flow rate was found to be 11.6 nm/s according to the change of apparent length of the copper core (Figure 3b). Accordingly, we calculated the mass change as shown in Figure 3c, and the mass flow rate can be then be determined by fitting the data to the curve $3 \times 10^{-9}t^2 - 1.2 \times 10^{-3}t + 0.12$, yielding approximately 120 ag/s, which is strikingly slow and well controllable, allowing precise delivery of mass at the attogram scale for time-based control that can readily reach subsecond precision.

Figure 3d shows time-resolved current vs voltage characteristics under a constant positive bias of 2.5 V. The current density under 2.5 V when flowing occurred was then calculated according to the cross sectional area as $2.60-3.07 \times 10^6$ A/cm^2. This is comparable to the observed value for electromigration of iron in CNTs (ca. 7×10^6 Å/cm^2).[21] The difference can be a result of the lower binding energy of copper to the carbon shells (0.1−0.144 eV/atom) than that of iron to carbon shells (0.3 eV/atom).[24] The high current densities employed here will lead to resistive heating. Temperatures as high as 2000−3000 °C have been estimated according to the lattice spacing change in electric breakdown experiments on nonfilled multiwalled nanotubes (MWNTs)[25] at a slightly higher bias (3 V) than those used here. We then correlated the current density J and the mass flow rate $\dot{m}$, as shown in Figure 3e. The relation $\dot{m} = 0.3135J^2 - 1.6206J + 2.1373$ suggests that a real positive value of $\dot{m}$ (≥ 42.9 ag/s) can only be given when the current density J surpasses 2.5847×10^6 A/cm^2. The existence of this threshold also implies the mechanism of the observed flowing is most possibly electromigration.[21] Under a negative bias, i.e., when the tungsten probe served as a cathode, we observed flow in the opposite direction.

Other possible mechanisms for flow can be excluded. Capillary force can induce filling/flowing, but the direction should be opposite to the observed flow, i.e., from the tip to the bottom of the carbon shells. Thermal expansion can enable flow, but the flow should be isotropic, heading toward
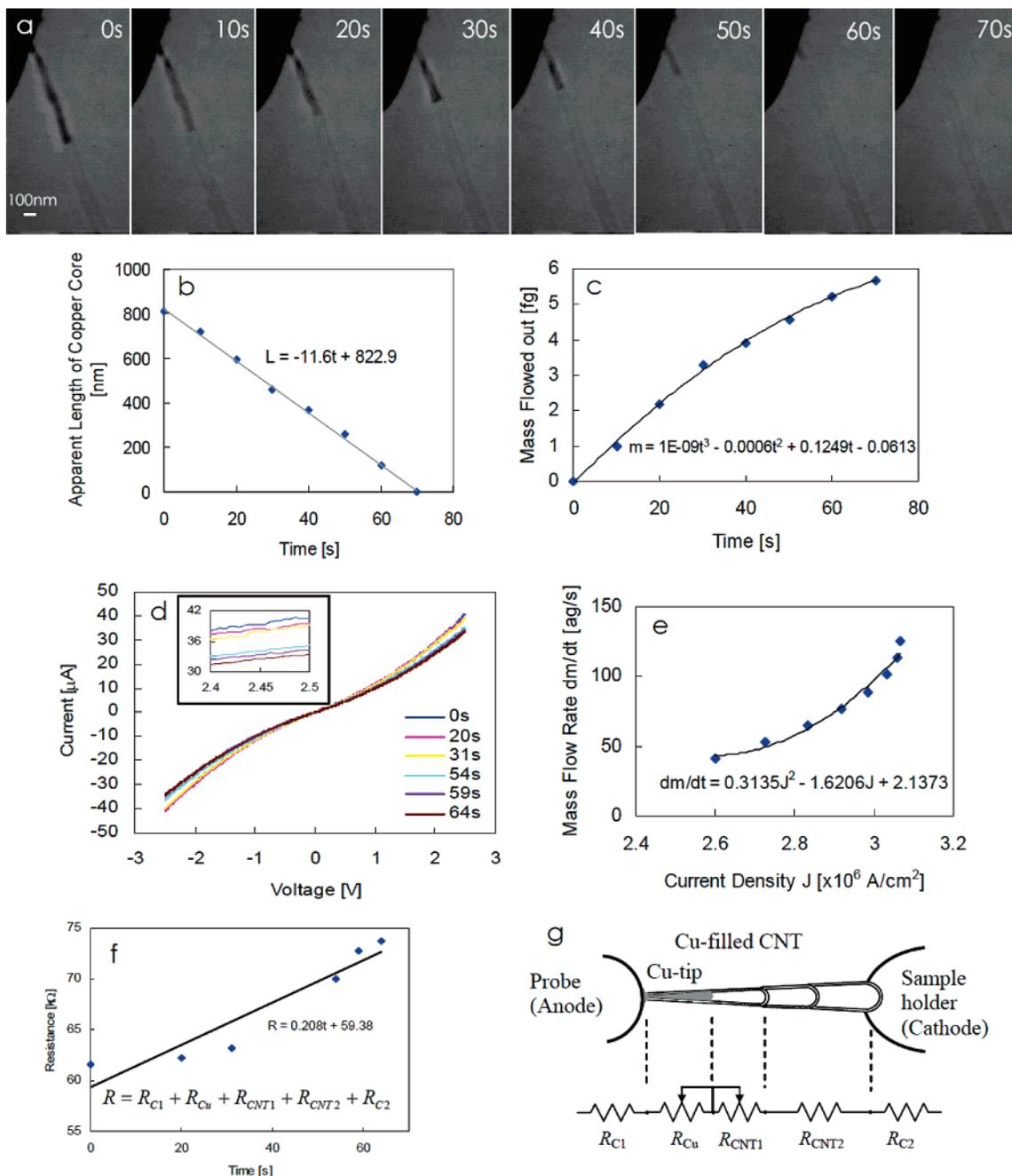
Figure 3. (a) Time-resolved TEM images from video frames showing the flowing process. The copper core started to flow inside the carbon shells from the root to the tip as the bias voltage reached up to 2.5 V. The whole process was continued for about 70 s. (b) The flow rate has been found to be 11.6 nm/s according to the change of apparent length of the copper core. The tungsten probe has been positively biased. (c) The mass changes along the time. The mass flow rate can be then drawn out from the fitting curve as approximately 0.12 fg/s. (d) Time-resolved current vs voltage characteristics under a constant bias of 2.5 V. The current density under 2.5 V as flowing occurred is about $2.60-3.07 \times 10^6$ A/cm². (e) Correlation of the current density J and the mass flow rate $\dot{m}$. (f) Time-resolved resistance changes under 2.5 V as flowing occurring (taken from (c)). (g) Electric circuit model of the Cu-filled CNT.

both the tip and the bottom. A recent investigation showed that the irradiation of MWNTs can cause a large pressure buildup within the nanotube core that can plastically deform, extrude, and break encapsulated solid material.[26] In our experiments, however, no contraction of the carbon shells was observed.

Figure 3f shows time-resolved resistance changes under 2.5 V as flowing occurred (taken from Figure 3d). The circuit resistance is composed of five parts shown schematically in

Figure 3g, i.e., the contact resistance between the copper tip and the probe, R_{C1}, the resistance of the copper core, R_{Cu}, the resistance of the first section of carbon shell without copper, R_{CNT1}, the resistance of the other sections of the nanotubes, R_{CNT2}, and the contact resistance between the CNT and the sample holder, R_{C2}. Note that the carbon shell with a copper core is in fact shortened by the copper core. Hence, the measured resistance is $R = R_{C1} + R_{Cu} + R_{CNT1} + R_{CNT2} + R_{C2}$. At $t = 0$ s, the first section of the Cu-filled CNT had

a copper core of 822.9 nm according to the fit value shown in Figure 3b, so the total resistance will exclude the R_{CNT1}, i.e., $R_{t=0} = R_{C1} + R_{Cu} + R_{CNT2} + R_{C2}$. Similarly, at $t = 70.9$ s, the entire copper core flowed out. In this case, the total resistance will exclude R_{Cu}, i.e., $R_{t=70.9s} = R_{C1} + R_{CNT1} + R_{CNT2} + R_{C2}$. According to the value fit in Figure 3f, $R_{t=0s} = 59.38$ kΩ and $R_{t=70.9s} = 73.94$ kΩ. The difference (14.75 kΩ) equals the resistance of the full length of the carbon shell in the first section without copper and that of the full length copper core. Because the resistivity of copper (1.57 × 10^{-8} Ωm) is sufficiently smaller than that of CNTs (on the order of 10^{-6} Ωm),[27] it is reasonable to ignore the resistance of copper in the difference. Hence, we can extract the resistance of the carbon shells from the measured circuit resistance. The increase of the resistance along with time is mainly caused by the shortening of the low resistant copper core and, accordingly, the continuous exposure of the highly resistant carbon shells. The resistivity of the carbon shells can thus be worked out as 1.6 × 10^{-6} Ωm according to the resistance (14.75 kΩ) and the average cross area of the shell (91 nm^2). This is a value smaller than that of natural graphite (1.4 × 10^{-5} Ωm)[28] and four-point measurements of supported, unfilled MWNTs (9.0 × 10^{-6} Ωm),[27] suggesting that multiple layers have been involved in carrying the current because of the end contact established between the CNT tip and the tungsten probe. It should be noted that, though we used two-terminal measurement, the resistance of the carbon shells originally with copper inside has been successfully identified due to the flowing of the copper, which provides a new method for extracting the resistance of a component from a measured circuit resistance without involving four-terminal measurement. This is particularly useful for the investigation of heterostructures such as those metal-filled CNTs provide when they have sufficiently different resistivities and melting points. It can also be found that the absolute value of the current at 1.5 V is about 1 order-of-magnitude larger than that shown in Figure 2f, which can be attributed to the improvement of the contact resistance between the CNT-tip and the tungsten probe due to the melted copper. Although we have no way of measuring the actual temperature of the nanotubes or the copper core, this process provides the possibility for estimating the temperature according to the resistivity change if we apply Matthissen's rule on temperature dependence of resistivity, provided that we know the resistivity at a certain temperature. Unfortunately, the latter is unknown. However, it has been noted that the temperature for CNT growth from 100 nm scale Cu particles in our synthesis (700 °C) is far lower than the melting point of bulk Cu (1083 °C).[22] It is well-known that the surface-to-volume ratio with respect to a nanosized particle can affect the melting point. Although the exact reason for melting at such a low temperature is not yet known, we have a rough estimation of the melting point of the copper core, i.e., around 700 °C. This is comparable to the in situ electron microscope observations of the melting point of the encapsulated 20−60 nm diameter Cu nanocrystals in multilayer graphitic carbon spheres, which was reported at 802 °C.[29] We also know according to the

experiment that the melting point of the carbon shells is much higher than that of the copper core. This provides further evidence of molten copper inside carbon shells.

The application of such controlled transportation of the copper core was then investigated. Self-soldering of CNTs with copper encapsulated in a CNT is shown in Figure 4. A copper-filled tube, CNT_1, was first attached to a tungsten probe (Figure 4a). A section of CNT_1 was then attached to and soldered onto CNT_2 by the melted copper (Figure 4b). Parts c−h of Figure 4 are video frames showing the soldering process. A copper-filled tube, CNT_1, was attached to a probe and brought into contact with another tube, CNT_2. The probe has a −10 V bias. Parts c−e of Figure 4 show three different positions as the probe was approaching CNT_2, and Figure 4f shows how contact has been made. The shape change of the copper suggests a melting process has occurred. It has been found from the video frames (25 fps) that the melting of the copper happened in a very short interval (<70 ms). With a higher bias (−15 V), CNT_1 was broken (Figure 4g) and its end section remained soldered to the tip of CNT_2 (Figure 4h). Besides self-soldering, other applications can include soldering other objects (Figure 4i,j) and thermal dip-pen lithography (T-DPL) for wiring/structuring (Figure 4k).

Compared with the other interconnection processes previously investigated, electrically driven spot welding has several interesting aspects: (i) A very low current can induce the melting and drive the flow, which is much more efficient than irradiation-based techniques involving high-energy electron beams,[7,9,26,30,31] FIB,[8] or lasers.[13] Combined with dielectrophoretic assembly, it is possible to solder the tubes onto electrodes for batch fabrication of NEMS. (ii) The welding site can be readily selected using nanorobotic manipulation, which enables 3D position and orientation control for continuous mass delivery and will potentially enable 3D prototyping and assembly. (iii) The melting occurs rapidly (at least at the millisecond level), several orders-of-magnitude faster than using high-intensity electron-beam or FIB, which is generally on the order of a minute.[7−9,26,31] (iv) Because both the rate and direction of mass transport depends on the external electrical drive, precise control of an ultrasmall mass delivery is possible. Time-based control will allow the delivery of attograms of mass.[32] (v) Copper has good compatibility in the conventional semiconductor industry. Our experiments show that it will likewise play an important role for scaled down systems. Carbon shells provide an effective barrier against oxidation and consequently ensure a long-term stability of the copper core, which also facilitates the conservation of the material than conveying mass on the external surface of nanotubes.[32]

In summary, spot welding using single-crystalline-copper-filled CNTs has been investigated experimentally using nanorobotic manipulation inside a TEM. Controlled melting and flowing of copper inside nanotube shells have been realized by applying a bias voltage of as low as 1.5 and 2.5 V, respectively. The melting is a result of Joule heating, whereas the flowing is caused by electromigration. The flow rate of the copper has been found to be 11.6 nm/s under a 2.5 V bias using time-resolved TEM images, which is
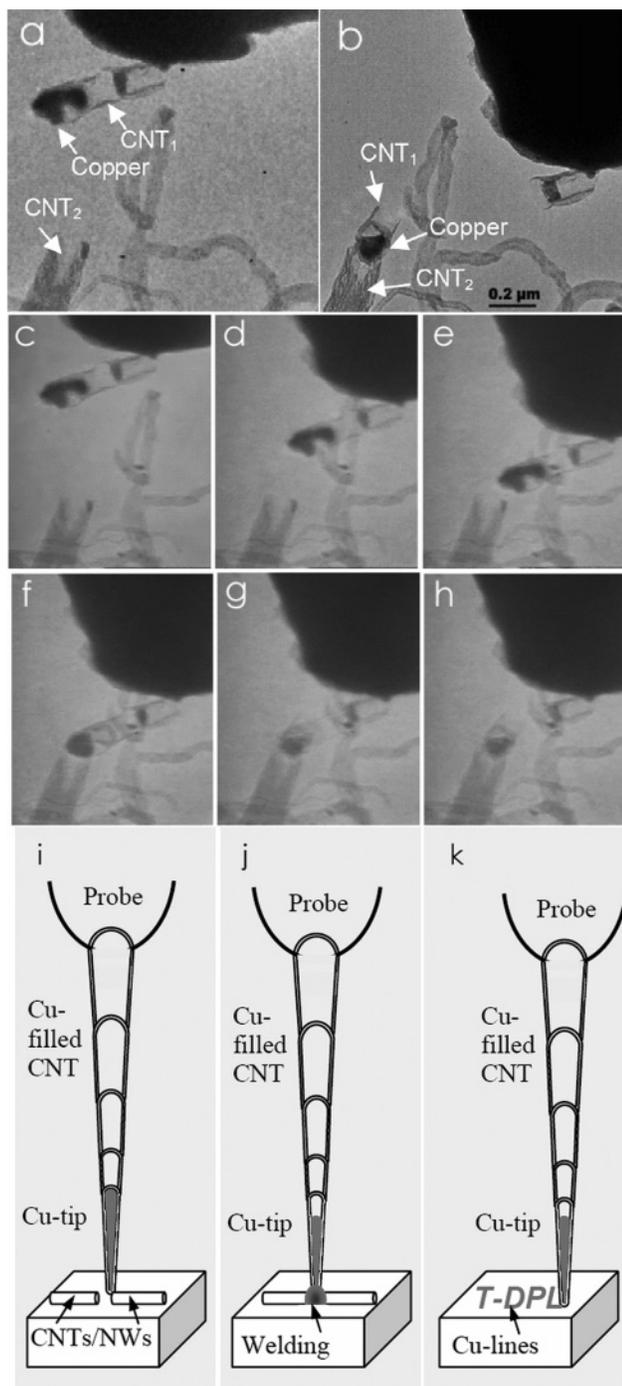
Figure 4. Self-soldering of CNTs with copper encapsulated in a CNT. (a) A copper-filled tube, CNT_1, was attached to a tungsten probe. (b) A section of CNT_1 was soldered onto CNT_2 by the melted copper. (c−h) Video frames showing the soldering process. A copper-filled tube, CNT_1, was first attached to a probe and brought into contact with another tube, CNT_2. The probe (cathode) has a -10 V bias. (c−e) Three different positions as the probe is approaching CNT_2. (f) Showing how contact has been made. The shape change of the copper suggested a melting process has occurred. With a higher bias (-15 V), CNT_1 was broken (g) and its end section remains soldered to the tip of CNT_2 (h). Besides self-soldering, other applications can include soldering other objects (i and j), thermal dip-pen lithography for wiring/structuring (k), etc.

strikingly slow and well controllable, allowing precise delivery of mass. The mass flow rate has been determined

to be 120 ag/s. A successful demonstration of self-soldering a copper-filled CNT onto another CNT shows promising for nano spot welding and thermal dip-pen lithography.

Supporting Information Available: Videos 1 and 2 (AVI) record the controlled flowing and soldering processes. This material is available free of charge via the Internet at http://pubs.acs.org.

References

(1) Cary, H. B.; Helzer, S. C. *Modern Welding Technology*, 6th ed.; Prentice Hall: Upper Saddle River, NJ, 2005; pp 4−10.
(2) Iijima, S. *Nature* **1991**, *354*, 56−58.
(3) Morales, A. M.; Lieber, C. M. *Science* **1998**, *279*, 208−211.
(4) Pan, Z. W.; Dai, Z. R.; Wang, Z. L. *Science* **2001**, *291*, 1947−1949.
(5) Zhang, L.; Ruh, E.; Grützmacher, D.; Dong, L. X.; Bell, D. J.; Nelson, B. J.; Schönenberger, C. *Nano Lett.* **2006**, *6*, 1311−1317.
(6) Dong, L. X.; Arai, F.; Fukuda, T. *IEEE-ASME Trans. Mechatron.* **2004**, *9*, 350−357.
(7) Dong, L. X.; Arai, F.; Fukuda, T. *Appl. Phys. Lett.* **2002**, *81*, 1919−1921.
(8) Matsui, S.; Kaito, T.; Fujita, J.; Komuro, M.; Kanda, K.; Haruyama, Y. *J. Vac. Sci. Technol., B* **2000**, *18*, 3181−3184.
(9) Xu, S. Y.; Tian, M. L.; Wang, J. G.; Xu, J.; Redwing, J. M.; Chan, M. H. W. *Small* **2005**, *1*, 1221−1229.
(10) Hirayama, H.; Kawamoto, Y.; Ohshima, Y.; Takayanagi, K. *Appl. Phys. Lett.* **2001**, *79*, 1169−1171.
(11) Dong, L. X.; Arai, F.; Fukuda, T. *Jpn. J. Appl. Phys., Part 1* **2003**, *42*, 295−298.
(12) Supple, S.; Quirke, N. *Phys. Rev. Lett.* **2003**, *90*, 214501.
(13) Kral, P.; Tomanek, D. *Phys. Rev. Lett.* **1999**, *82*, 5373−5376.
(14) Ajayan, P. M.; Iijima, S. *Nature* **1993**, *361*, 333−334.
(15) Tsang, S. C.; Chen, Y. K.; Harris, P. J. F.; Green, M. L. H. *Nature* **1994**, *372*, 159−162.
(16) Ajayan, P. M.; Colliex, C.; Lambert, J. M.; Bernier, P.; Barbedette, L.; Tence, M.; Stephan, O. *Phys. Rev. Lett.* **1994**, *72*, 1722−1725.
(17) Smith, B. W.; Monthioux, M.; Luzzi, D. E. *Nature* **1998**, *396*, 323−324.
(18) Ajayan, P. M.; Stephan, O.; Redlich, P.; Colliex, C. *Nature* **1995**, *375*, 564−567.
(19) Gao, Y. H.; Bando, Y. *Nature* **2002**, *415*, 599−599.
(20) Ugarte, D.; Chatelain, A.; de Heer, W. A. *Science* **1996**, *274*, 1897−1899.
(21) Svensson, K.; Olin, H.; Olsson, E. *Phys. Rev. Lett.* **2004**, *93*, 145901.
(22) Tao, X. Y.; Zhang, X. B.; Cheng, J. P.; Luo, Z. Q.; Zhou, S. M.; Liu, F. *Diamond Relat. Mater.* **2006**, *15*, 1271−1275.
(23) Svensson, K.; Jompol, Y.; Olin, H.; Olsson, E. *Rev. Sci. Instrum.* **2003**, *74*, 4945−4947.
(24) Weissmann, M.; García, G.; Kiwi, M.; Ramírez, R.; Fu, C.-C. *Phys. Rev. B* **2006**, *73*, 125435.
(25) Huang, J. Y.; Chen, S.; Jo, S. H.; Wang, Z.; Han, D. X.; Chen, G.; Dresselhaus, M. S.; Ren, Z. F. *Phys. Rev. Lett.* **2005**, *94*, 236802.
(26) Sun, L.; Banhart, F.; Krasheninnikov, A. V.; Rodrıguez-Manzo, J. A.; Terrones, M.; Ajayan, P. M. *Science* **2006**, *312*, 1199−1202.
(27) Schoenenberger, C.; Bachtold, A.; Strunk, C.; Salvetat, J.-P.; Forro, L. *Appl. Phys. A* **1999**, *69*, 283.
(28) *The CRC Handbook of Chemistry and Physics*, 70th ed.; Chemical Rubber Company: Cleveland, Ohio, 1990−1991.
(29) Schaper, A. K.; Phillipp, F.; Hou, H. *J. Mater. Res.* **2005**, *20*, 1844−1850.
(30) Madsen, D. N.; Molhave, K.; Mateiu, R.; Rasmussen, A. M.; Brorson, M.; Jacobsen, C. J. H.; Boggild, P. *Nano Lett.* **2003**, *3*, 47−49.
(31) Yokota, T.; Murayama, M.; Howe, J. M. *Phys. Rev. Lett.* **2003**, *91*, 265504.
(32) Regan, B. C.; Aloni, S.; Ritchie, R. O.; Dahmen, U.; Zettl, A. *Nature* **2004**, *428*, 924−927.

NL061980+

materials@nature.com

SEARCH   [go]   advanced search

Monday

nanozone news

20 December 2006

Spot-welding with nanotubes

There are several ways to join up carbon nanotubes into complex structures and 'circuit patterns' for nanoelectronics and nanomechanical systems. But a new metal spot-welding method has several advantages.

PHILIP BALL

If carbon nanotubes are to be the building blocks for nanoscale electronic circuits and nanoelectromechanical systems (NEMS), it will be useful to have a reliable way of joining them together — ideally via electrically conducting junctions. Bradley Nelson of ETH in Zürich, Switzerland, and his co-workers have found that nanotubes themselves supply the ideal tool for this kind of joinery[1].

They show that carbon nanotubes filled with copper metal can act as nanoscale spot welders. When electrically heated, the encapsulated metal melts and flows out, being delivered in a highly controllable manner with nanometre positional precision. The researchers have used this method to weld two nanotubes together.

Nanotubes and nanowires have been 'welded' before, for example using ion beams to deposit material or electron beams to 'melt' the graphitic carbon walls [2–4]. But these are an energy-intensive processes, and require rather complicated instrumentation. Nanotubes will also stick together purely from van der Waals forces[5], but the resultant join is weak.

Nelson and colleagues figured that, because the melting point of copper is rather modest, it might be possible to use copper-filled nanotubes as nanopipettes for delivering molten metal to well-defined locations. Nelson's colleagues at Zhejiang University in Hangzhou, China, have previously developed a method for preparing such filled nanotubes by chemical vapour deposition of carbon in the presence of a copper catalyst[6].

The nanotubes formed this way have tapering, needle-like tips with a

'bamboo' structure: they consist of nested carbon shells that are closed up at one end, with these endcaps spaced at intervals along the tube length, creating nanostructures reminiscent of the segmented form of bamboo. Only the tips tend to be filled with copper. The nanotubes were typically about 5 μm long, with diameters of 40–80 nm.

The researchers pasted a bundle of these tubes onto a gold wire with the needle-like tips pointing outwards. They could then use a tungsten probe tip, 200 nm across at the end, to make contact with an individual nanotube, while observing them through an electron microscope. They found that by applying a voltage between the probe and a nanotube while the two were in contact, the temperature could be raised past the melting point of copper by resistive heating.

This started to happen at a voltage of 1.5 V. At that point, the researchers saw a small vacant region, like a little bubble, open up in the copper held within the first conical 'bamboo' section of the nanotube. This empty space was caused by metal flowing out of the tube end onto the probe. The 'bubble' moved to the top end of the bamboo section, after which the meniscus of molten copper within the tube gradually descended towards the tip as the copper flowed out. Finally, the researchers detached the nanotube from the probe, with a small droplet of metal still stuck to the end. All the rest of the copper — an estimated 5.5 femtograms (5.5×10^{-15} g) – had diffused onto the probe.

Nelson and colleagues calculated that the flow rate at a voltage of 2.5 V was 120 attograms (120×10^{-18} g) per second — an extremely slow rate of discharge from the copper-filled nanotube, allowing for very precise control of the amount of material delivered from the tube.

But why does it flow out at all? Capillary action would lead to quite the reverse: material being drawn into the tube. The researchers believe that the copper is moved by electromigration in the presence of the electric field. When they charged the tungsten probe negatively rather than positively, they could induce flow in the other direction, supporting this idea.

The researchers also estimate that the encapsulated copper melts at a significantly lower temperature than the bulk metal — around 700 °C rather than 1,083 °C. This lower melting point for nanoscale metal particles is well known, and indeed 20–60 nm copper nanoparticles encapsulated in graphitic carbon spheres have been seen to melt at around 800 °C (ref. 7).

Nelson and colleagues decided to use this method to weld two nanotubes. They attached one of them, filled with copper at its tip, to the tungsten probe, and manipulated it to touch a second, empty tube. They then applied a voltage to the probe, and found that the nanotubes became joined by a blob of metal. When the first tube was broken by applying a higher voltage, its end remained stuck to the second nanotube.

The researchers say that among the attractions of this approach to joining nanotubes is that the energy needed is rather small (the voltages needed to melt the copper are low), the tubes can be positioned with great precision in three dimensions, the melting occurs rapidly, and the copper is protected against oxidation while it remains inside the nanotube. What's more, copper metal is already widely used for wiring microelectronic circuits, and so the method is compatible with existing chip technology. A copper-filled nanotube might alternatively be used as a kind of fountain pen to write out copper wiring at the nanoscale.

References

1. Dong L., Tao X., Zhang L., Zhang X. & Nelson B. J. Nanorobotic spot welding: controlled metal deposition with attogram precision from copper-filled carbon

nanotubes. *Nano Lett.* doi:10.1021/nl061980+ (2006)
Article

2. Matsui S. *et al.* Three-dimensional nanostructure fabrication by focused-ion-beam chemical vapor deposition. *J. Vac. Sci. Technol. B* **18,** 3181–3184 (2000)
Article

3. Krasheninnikov A. V., Nordlund K., Keinonen J. & Banhart F. Ion-irradiation-induced welding of nanotubes. *Phys. Rev. B* **66,** 245403 (2002)
Article

4. Xu S. Y. *et al.* Nanometer-scale modification and welding of silicon and metallic nanowires with a high-intensity electron beam. *Small* **1,** 1221–1229 (2005)
Article

5. Dong L. X., Arai F. & Fukuda T. Destructive constructions of nanostructures with carbon nanotubes through nanorobotic manipulation. *IEE-ASME Trans. Mechatron.* **9,** 350–357 (2004)
Article

6. Tao X. Y. *et al.* Thermal CVD synthesis of carbon nanotubes filled with single-crystalline Cu nanoneedles at tips. *Diamond Relat. Mater.* **15,** 1271–1275 (2006)
Article

7. Schaper A. K., Phillipp F. & Hou H. Melting behavior of copper nanocrystals encapsulated in onion-like carbon cage. *J. Mater. Res.* **20,** 1844–1850 (2005)
Article

molecules. Now, John Polanyi and co-workers at the University of Toronto in Canada have found that a single surface Si atom — an adatom — switches between low (off) and high (on) conducting states when an adjacent pair of molecules — a dimer — undergoes a change of configuration.

Scanning tunnelling microscopy (STM) showed that on/off currents and switching rates were dependent on whether the adatom was sitting directly above another Si atom (faulted) or not (unfaulted). The switching rate varies with temperature, which means that the activation energy for the process could be calculated. It is suggested that stabilization of the faulted 'on' state by its sub-surface Si atom leads to a high activation energy for 'on' to 'off' switching in this arrangement. Theoretical calculations identified two similar dimer structures that corresponded to energy minima. Simulated STM images of the 'on' and 'off' states using these structures closely resembled the experimental images.

The density of states at the faulted adatom is shifted down by 1 eV when the switch is off. This is consistent with changes in the local electric field induced by variation of the molecular configuration of the dimer. Moreover, the magnitude of this shift is similar to that achieved by doping a semiconductor.

MOLECULAR DEVICES
Rack and roll
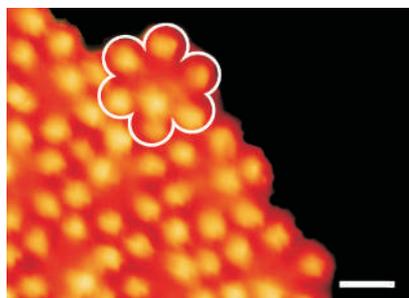
Nature Mater. **6,** 30–33 (2007)
Molecules designed to mimic the functions of macroscopic machines are often studied as large ensembles in which their individual characteristics are not observed directly. In this way, the precise atomic-scale motions of the components of such systems remain hidden amongst averaged overall behaviour.

Now, researchers in France and Germany have looked at a molecular 'rack-and-pinion' device in which a single molecule (the pinion) — reminiscent of a six-toothed cog — can be moved

along the edge of a molecular island (the rack) comprising many copies of the same compound. Christian Joachim and colleagues from CEMES-CNRS in Toulouse and the Freie Universität Berlin used a scanning tunnelling microscope (STM) to move a molecular cog along the serrated edge of a self-assembled island on a Cu surface. The STM tip was placed above the centre of a single cog, pinning the molecule to the surface while still allowing it to rotate about its central axis. As the tip was displaced along the island's border, the cog moved with it to the next position along the 'rack'.

One tooth of the cog had a different structure to the others so could be distinguished during imaging and from this it could be seen that the displacements along the 'rack' resulted in successive 60° rotations of the cog.

GLUCOSE SENSING
Silicon's sweet spot

Appl. Phys. Lett. **89,** 243901 (2006)
Diabetes is a metabolic disorder that is characterized by the body's inability to regulate blood sugar levels. Considerable effort is expended on the development of fast, reliable and economical glucose sensors. Conventional electrochemical sensors use glucose oxidase — an enzyme — as the sensing element, but these are unstable under physiological conditions. Alternative enzyme-free sensors made using noble metals suffer from other deficiencies, such as electrode poisoning.

Now, Siu-Tung Yau and colleagues from Cleveland State University and the University of Illinois at Urbana-Champaign in the USA have made a high performance enzyme-free glucose sensor using 1-nm-sized silicon particles. Si_{29} particles were synthesized by the electrochemical etching of crystalline silicon and were then deposited on silicon substrates to act as Si_{29}–Si sensing elements. The Si_{29} particles act as catalysts for the oxidation of glucose and relay the electrical signal to the silicon electrode. A linear response for glucose levels up to 50 mM was observed.

The Si_{29}–Si electrode sensors did not suffer from electrode poisoning, were stable after repeated use over a 14-day period, and exhibited a four-fold enhancement response when compared with glucose oxidase based sensors. The superior performance of the silicon-based sensors is thought to arise from enhanced accessibility of the glucose to the Si_{29} particles and shorter electron tunnelling distances than in enzyme-based sensors.

TOP DOWN BOTTOM UP
Making connections

Researchers in robotics and materials science can solder components at the nanoscale.

After presenting at the NanoChina 2005 conference in Beijing, Lixin Dong from the Institute of Robotics and Intelligent Systems (IRIS) at ETH Zurich, Switzerland was approached by Xinyong Tao, a PhD student in materials science at Zhejiang University in Hangzhou, China. Tao was fascinated by the way nanorobots could manoeuvre individual nanostructures so they could be studied, and Dong agreed to characterize the field-emission properties of the copper-tipped carbon nanotubes that Tao had made.

Dong's initial measurements showed that the copper-tipped nanotubes did have better field-emission properties, as expected. But then he noticed something surprising: when a lower voltage was applied to the nanotubes over an extended period of time, it was possible to keep the nanotubes intact while allowing the copper to melt and flow out. Using a nanorobotic manipulator inside an electron microscope, the collaboration went on to show that the copper-tipped nanotubes could solder nanotubes together in a nanosized version of assembly lines found in the automobile industry (*Nano Lett.* **7,** 58–63; 2007).

"Bottom-up collaboration is often more effective than the top-down approach because the motivation is purely for the thrill of science, rather than simply to obtain additional funding", says Bradley Nelson, director of the IRIS lab in Zurich. He adds that this collaboration was not officially funded and relied instead on existing grants at IRIS and Xiaobin Zhang's laboratory at Zhejiang University.

Bradley has started several collaborations as a result of discussions at conferences. "Oral presentations are incredibly important because this is where strong impressions are made on the quality of the work and group," he says. "Don't be afraid to email authors of papers that are of interest, and don't worry about who gets credit, or where the funding will come from. With good work, there will be plenty of credit to go around, and avenues to apply for additional funding."

The definitive versions of these Research Highlights first appeared on the *Nature Nanotechnology* website, along with other articles that will not appear in print. If citing these articles, please refer to the web version.